17th World Conference on Earthquake Engineering, 17WCEE
Sendai, Japan - September 13th to 18th 2020

INFLUENCE OF VERTICAL MASSES ON THE RESPONSE OF GRAVITY-CONTROLLED ROCKING BRACED FRAMES

P. Mottier [1], R. Tremblay [2], C. A. Rogers [3], L. Wiebe [4]

[1] *Ph. D. Candidate, Dept. of Civil, Geological and Mining Engineering, Polytechnique Montreal, Montreal, QC, Canada, paul.mottier@polymtl.ca*
[2] *Professor, Dept. of Civil, Geological and Mining Engineering, Polytechnique Montreal, Montreal, QC, Canada, robert.tremblay@polymtl.ca*
[3] *Professor, Dept. of Civil Engineering and Applied Mechanics, McGill University, Montreal, QC, Canada, colin.rogers@mcgill.ca*
[4] *Associate Professor, Dept of Civil Engineering, McMaster University, Hamilton, ON, Canada, wiebel@mcmaster.ca*

Abstract

The implementation of rocking systems is considered as an efficient way to design resilient buildings or to retrofit seismically deficient ones, as it reduces the amount of lateral seismic forces applied to the building. In a controlled-rocking braced frame system (CRBF), the columns of the braced frames are designed to uplift from their foundations. Re-centring capacity of the building may be provided by adding vertical post-tensioning elements, the gravity loads supported by the braced frames or by a combination of these elements. When the self-centring capacity is solely conferred by the tributary gravity loads of the frames, CRBFs are referred to as gravity-controlled rocking braced frames (G-CRBF). Energy dissipative devices (ED) can also be implemented on the frame (at the column base, for instance) to control drifts. The rocking frame hence exhibits a typical flag-shaped overturning moment – base rotation hysteretic behaviour during a major earthquake event. Two different numerical analysis approaches have been used in past research to study the overall response of rocking braced frames subjected to ground motions. The first approach is based on a 2D-model of rocking braced frames. Frame members are modelled using elastic beam column elements and vertical masses are added to joints to replicate the masses carried by the frame. An ED device is modelled by a nonlinear element and placed between the foundation and the column base plates. A leaning column is linked to the model to capture P-Delta effects. The second approach consists of the use of a single-degree-of-freedom (SDOF) model using a self-centring material calibrated to produce the same hysteresis as the system under quasi-static loading. The study was then extended to rocking frames for buildings of up to 5 storeys. In this case, two identical complete frame models were used except that only one model included the vertical masses.

A comparative study between the seismic responses obtained with the use of these two numerical analysis approaches is presented in this paper in order to examine the effects of the vertical masses on the behaviour of the structure. Single-storey chevron bracing is used as the rocking frame design and the ED device is selected to be friction based. Parameters used for the self-centring material are chosen to be equivalent to those selected for the rocking braced frame. The key difference between the two models mentioned is the ability to capture inertia effects due to rocking and induced by the vertical masses added to the joints of the 2D-model. Nonlinear analyses are then performed using the OpenSees software. Ground motions representative of the seismic hazard in Vancouver, BC, are scaled and used to compare the responses of the two numerical models. Focus is put on the drift demands, as well as on the vertical base reactions and the horizontal base shear. For single-storey frame, the results showed overall similar drift histories, but the G-CRBF model with vertical masses experienced smaller peak drift values than the SDOF model without vertical masses. Larger force demands were however observed in the G-CRBF model due to the response associated to the structure vertical vibration mode when one column is uplifted. The results also showed that these differences still exist in multi-storey rocking frames but the effects of the vertical masses on the overall response of G-CRBFs tend to be relatively less significant as the number of storeys is increased.

Keywords: Seismic design; Braced steel frames; Rocking; Column Impact; Column uplift; Vertical mass

1. Introduction

The use of controlled-rocking braced frame (CRBF) systems can bring resilience and safety to steel structures subjected to major earthquakes. Such structures have been studied for several decades [1], proving that the ability for a structure to rock on its foundation is an efficient way to reduce the lateral seismic forces transferred to the structure during an earthquake, thus reducing the demands on the frame members without residual drifts. Several shake table studies have been conducted and have proved the efficiency of the system [2-4]. Guidelines and design methods have been developed following these studies [5-6]. However, these methods focused on rocking structures that rely on the use of post-tensioning (PT) strands to re-centre the building. In this configuration, the floor system is decoupled from the CRBF in the vertical direction. Most guidelines that have been developed for the design of such structures are based on a 2-D CRBF models in which all framing members are modelled using elastic beam-column elements [7]. In order to simplify the computational work, other guidelines for the design of PT and ED elements are based on an equivalent single-degree-of-freedom (SDOF) model to mimic the global dynamic behaviour of the rocking structures [8-9]. In this case, the SDOF properties are selected to match the lateral stiffness of the building as well as the ED properties, when applicable.

Rocking structures may also rely on gravity loads alone to re-centre the building, referred to as gravity-controlled rocking braced frame (G-CRBF) structures. In that case, the floor system must be connected to the CRBFs in the building. As a consequence, the coupling effect between the lateral- and vertical-load resisting systems results in amplified impacts between the rocking columns and their foundations. When these columns return to their original position, vertical inertia forces are triggered in the frame members. Gravity-controlled rocking braced frames have been recently studied; the initial numerical modelling results indicate promising performance under seismic excitation [10-11]. These studies have used the 2-D modelling approach in order to capture the inertia effect due to the vertical masses carried by the frame. Another numerical study [12] evaluated the feasibility of a using simplified SDOF model to analyze a 4-storey G-CRBF, concluding on the reasonable accuracy of such a method to predict the floor displacements, drifts and base shear demands.

A comparative study between the seismic responses obtained for a G-CRBF building modelled with a 2-D frame carrying vertical masses and an equivalent SDOF approach is presented herein. The purpose is to identify how the previously mentioned guidelines could be applied to the design of G-CRBF buildings. To do so, several buildings located in Vancouver, BC, are modelled according to the two different approaches. In order to understand the behaviour of the building, the study firstly concentrates on a single-storey building. Nonlinear analyses are then performed using the OpenSees [13] software. Ground motions representative of the seismic hazard in Vancouver, British Columbia, are scaled to the 2015 National Building Code of Canada (NBCC) design spectrum [14-15] and used to assess the response of the two numerical models. The results of the analyses are used to compare the global behaviour of the studied building. Focus is being put on the vertical base reactions and horizontal base shears. Differences between roof drifts are also investigated. The study is then expanded to examine different building heights.

2. Definition of the numerical models

A single-storey building located in Vancouver, BC, is considered for the first analysis. Typical member sizes were considered as brace-, beam- and column-sections to obtain a realistic value of the fundamental period of vibration. A plan view is given in Fig. 1. he seismic weight was equal to 2600 kN, assuming roof dead load ω_{Dead} = 3.6 kPa and the weight of exterior walls taken equal to ω_{Wall} = 0.5 kPa. The initial period of the fixed-base structure was equal to T_{init} = 0.343 s. The frame was modelled using OpenSees [13]. A schematic description of the two models is displayed in Fig. 2. The 2-D G-CRBF model (Fig. 2a), later described as G-CRBF, was assembled assuming a linear elastic response of the frame members during the earthquake; hence, all the frame members were represented using elastic truss elements. Uplift was modelled using gap elements with a compression stiffness equal to the axial stiffness of the column of the frame at the rocking connection amplified by a factor of 10.8. The reaction blockers were modelled as horizontal gap elements with the same axial stiffness as the vertical gap elements. Energy dissipative (ED) devices were added at the bases of the

columns as friction devices modelled as elastic-perfectly plastic elements with a yielding force being equal to their activation force F_s. F_s was considered equal to 0.5 times the total gravity load carried by one column: F_s = 0.5 P. For the structure studied, moment equilibrium about the rocking joint gives the value of the static base shear V_R required to initiate column uplift:

$$V_R = (P + F_s)\, L/h = (125 + 62.5)\, 7.6/5.4 = 263 \text{ kN} \quad (1)$$

where P is the tributary gravity load of the uplifted column, F_S is the activation force of the ED device, and L and h are respectively the width and the height of the frame. This corresponds to a response modification factor R = 8 when compared to the elastic demand from NBC 2015 design spectrum [15]. The lateral seismic weight was applied as a lumped mass m_h assigned to the node at the mid-span of the roof beam. Dead loads were applied as concentrated loads P at the column top-nodes that were determined from the tributary area of the columns. To account for the inertia forces induced by the distributed mass on the uplifted beams, consistent vertical masses m_v obtained assuming rigid beams displaced upwards at the column lines were added at the top of each column of the CRBF. Assuming a braced frame located in the E-W direction and secondary beams installed at a spacing of $L/3$, m_v is the total consistent mass contributed by the two edge beams, $m_{v,edge}$, and the main girder, $m_{v,girder}$:

$$m_{v,edge} = 1/3 \times (\omega_{Dead}\, L^2/6 + \omega_{Wall}\, Lh\,) = 18.4 \text{ kN} \quad (2)$$

$$m_{v,\,girder} = 2 \times 1/3 \times (\omega_{Dead}\, L^2/3) \times 1/3 + 2 \times 1/3 \times (\omega_{Dead}\, L^2/3) \times 2/3 = 46.2 \text{ kN} \quad (3)$$

$$m_v = 2 \times m_{v,edge} + m_{v,girder} = 83 \text{ kN} \quad (4)$$

where L is the width of the frame and h is the height of the frame.

P-Delta effects were captured using an adjacent leaning column with the top node lateral displacement being constrained to that of the mid-span node of the frame. That leaning column was modelled using a truss element with an area section equal to the sum of the cross-section areas of the columns within the lateral tributary area of the considered braced frame. The vertical load applied on the leaning column was set equal to the total gravity load applied on the lateral tributary area of the braced frame P_{grav}, reduced by the vertical loads already applied on the braced frame columns.

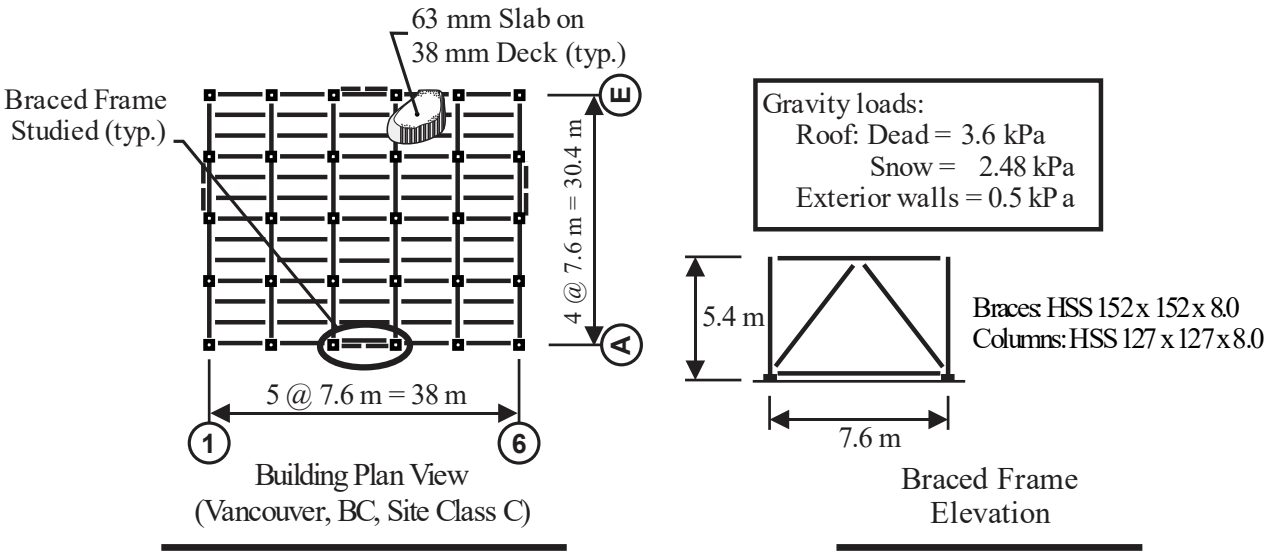

Fig. 1 Building Plan View

The SDOF system in Fig. 2b was modelled using a truss element column laterally braced by a horizontal spring. The spring was assigned a self-centring material with the same lateral stiffness, energy dissipation and lateral capacity from column uplift as the G-CRBF of Fig. 2a. The horizontal mass m_h was assigned at the column top node and total load P_{grav} was applied to the column to include P-Delta effects on the response.

In both models, mass-proportional damping was assigned to the horizontal mass m_h assuming a damping ratio of 3% of critical damping in the horizontal mode of the fixed-base frame. This created a damping ratio of respectively 0.85% and 0.44% in the vertical modes of the frame associated to periods $T_{u,v}$ and T_c that will be introduced in section 3.

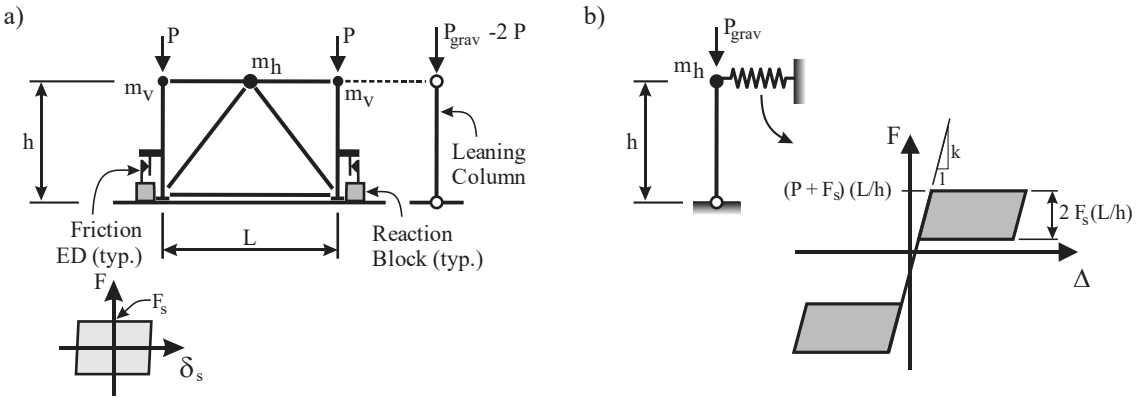

Fig. 2 Numerical models used for the 1-storey building analyses: a) 2-D G-CRBF with vertical masses; b) Equivalent SDOF system.

3. Response to example ground motion: comparison between SDOF and G-CRBF

Each numerical model was subjected to 11 ground motions from crustal earthquakes contributing to the seismic hazard of the region of Vancouver, BC. The selected ground motions were scaled according to the guidelines of the 2015 NBC [15]. The characteristics of the ground motions, as well as the scaling factor *SF1* as defined in [15], are detailed in Table 1. *SF2* was equal to 1.025

Table 1 Characteristics and scaling factors of the selected crustal ground motion records

GM ID	Earthquake	Year	M_w	Record No.	Comp.	R (km)	V_{s30} (m/s)	SF1
1	"San Fernando"	1971	6.61	57	291°	19.33	450	1.352
2	"Imperial Valley-06"	1979	6.53	164	237°	15.19	472	1.636
3	"Corinth_ Greece"	1981	6.6	313	L	10.27	361	1.378
4	"Loma Prieta"	1989	6.93	769	60°	17.92	663	2.78
5	"Loma Prieta"	1989	6.93	801	315°	14.18	672	1.573
6	"Northridge-01"	1994	6.69	963	90°	20.11	450	0.659
7	"Northridge-01"	1994	6.69	986	195°	12.92	417	1.774
8	"Northridge-01"	1994	6.69	989	70°	9.87	740	1.517
9	"Northridge-01"	1994	6.69	1083	170°	12.38	402	2.409
10	"Chuetsu-oki_ Japan"	2007	6.8	4841	NS	20.65	655	1.842
11	"Chuetsu-oki_ Japan"	2007	6.8	4864	NS	4.69	655	0.998

The response from the two numerical models for ground motion #6, which is representative of the overall results, is shown in Fig. 3. The results are presented from bottom to top, the ground motion signal being presented at the bottom of the figure and the response of the structure above. In Fig. 3, vertical lines have been plotted to identify the times at key lateral displacements during the largest column uplift excursion. From left to right, the four lines indicate, respectively, initiation of the column uplift in the SDOF model (t = 12.86 s) and in the G-CRBF model (t = 12.94 s), peak lateral displacement (t = 13.34 s), and the end of column uplift in the two models (t = 13.75 s).

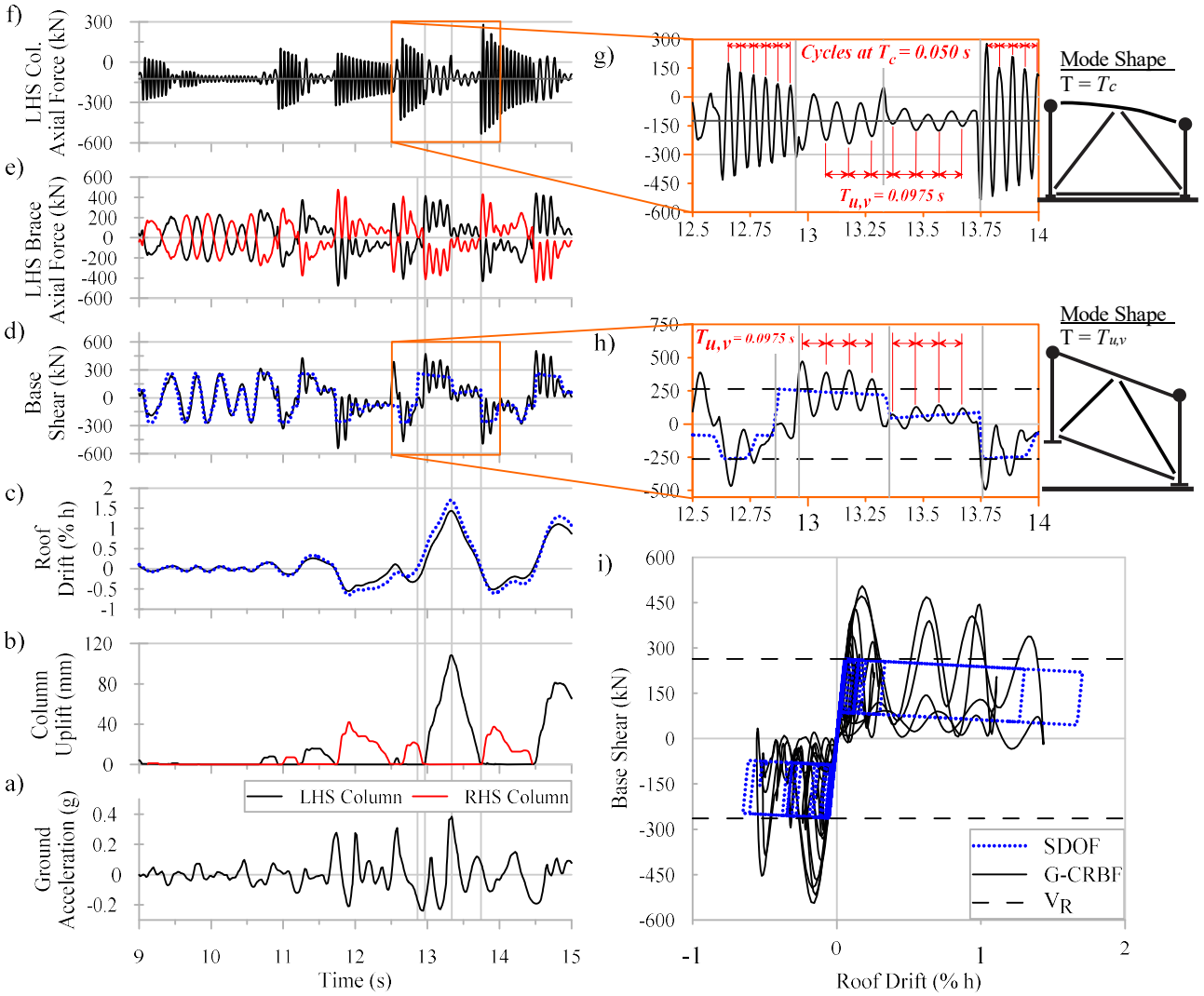

Fig. 3 Comparison of the response history analysis results from the G-CRBF and the SDOF models: a) Ground motion; b) Column uplift; c) Roof drift; d) & h) Base shear; e) Brace axial load; f) & g) Column axial load; i) Base shear *vs.* roof drift hysteresis.

Fig. 3b displays the vertical uplift of the left-hand side (LHS) and right-hand side (RHS) columns of the G-CRBF. Fig. 3c shows that the ground motion triggers generally similar response in roof displacement histories with both models, but the values of peak displacements obtained with the SDOF model are approximately 10% higher than those obtained with the G-CRBF model. Moreover, for significant uplifts, the duration of the rocking cycles is modified. For example, the biggest uplift cycle lasts 0.81 s for the G-CRBF model, but 0.88 s for the SDOF model, which represents an 8 % increase. Such a difference is attributed to the fact that part of the input energy is used to lift the vertical masses carried by the frame, which is not the case in the SDOF model. As a result, more energy is available in the SDOF model to induce lateral displacements.

Fig. 3d and h display the computed base shear history. As can be seen, before the initiation of rocking in the building (t < 10.5 s), the base shear in both models remains within V_R. However, after rocking has started, the base shear response starts to oscillate with significant peaks in the G-CRBF model, these peaks occurring at the beginning of each column uplift excursion.

Fig. 3h displays a magnified view of the base shear history in the two models. As can be seen, the two models present similar behaviour, on average, but the G-CRBF model exhibits oscillations in base shear not present in the SDOF model. For the latter, as soon as the hysteretic cycle starts at t = 12.86 s, the base shear is equal to V_R. It then gradually decreases during the upward motion of the frame due to -Delta effects. At t = 13.34 s, the peak uplift is reached, and the column begins returning downwards to its original position. The base shear immediately decreases by 2 F_S (L/h) = 176 kN due to slip reversal the ED device, and then slightly increases again, due to P-Delta effects reducing as the displacement diminishes, to reach $V_{R,\,Down} = V_R - 2\,F_S\,(L/h)$ = 88 kN. At t = 13.75 s, the uplift cycle is completed, and the base shear is then equal to $-V_R$, as the opposite column has started to uplift. In the same time period, the base shear measured in the G-CRBF model varies significantly. During the uplifting phase, from t = 12.94 s to t = 13.34 s, the base shear oscillates around the static value V_R = 263 kN, ranging from 57 kN (0.21 V_R) to 463 kN (1.76 V_R). Between t = 13.34 s and t = 13.75 s the LHS column moves downwards; the base shear then decreases and oscillates around the static value $V_{R,\,Down}$, between -34 kN (-0.38 $V_{R,\,Down}$) and 143 kN (1.63 $V_{R,\,Down}$). Then, the RHS column is uplifted and the base shear oscillates around $-V_R$. Fig. 3h shows that the base shear oscillations have a period of 0.0975 s, which corresponds to the period of the vertical mode of the frame during column uplift, $T_{u,v}$, as obtained from a modal analysis [16]. The mode shape associated with that period is schematically drawn on the right of the figure. As plotted in Fig. 3e, axial loads in the braces exhibit the same behaviour as the base shear and the same oscillations at the period $T_{u,v}$ can be observed. As for the base shear, oscillations at the period $T_{u,v}$ can be seen after rocking has been initiated in the structure at t = 10.5 s; before that time, the force demands are governed by the first mode of the structure (T_{init}).

The axial force in the LHS column of the G-CRBF is plotted in Fig. 3f. A magnified view of this history is presented in Fig. 3g. Before t = 10.5 s, the G-CRBF behaves as a regular pinned-base structure and the column force oscillates with significant variations around the static value P at a period of 0.050 s, which corresponds to the period of the column axial vibration mode, T_c. When the rocking of the LHS column is initiated, the compression force oscillates around P at the period $T_{u,v}$. As soon as the LHS column returns to its original position, the column force suddenly increases due to column impact. At t = 13.75 s, the compression force reaches a maximum value of 534 kN, which reveals that the vertical masses increase the column axial load by up to 4.27 times the static value P. The same behaviour is observed for the RHS column, but it is not plotted for clarity.

The oscillations that are observed in the brace axial load, base shear and column axial load responses are a consequence of vibrations of the vertical masses carried by the uplifted rocking columns. These vibrations are triggered by the sudden change in boundary condition that occurs when the column base starts uplifting. Before uplifting, because of the vertical mass present at the column top , the column functions as a fixed-base vertical spring that oscillates at period T_c as long as it remains in contact with the foundation. When uplift starts, the column base is released, and the vertical mass starts vibrating vertically at the period $T_{u,v}$ because the vertical rocking mode of the frame upon column uplift is activated. That vibration of the mass is transferred to the horizontal mass m_h through the brace that is uplifted from its initial position, for the duration of the uplift excursion, which explains why the base shear oscillate at the period $T_{u,v}$ when the frame is rocking. In contrast, when no vertical mass is assigned at the column tops, the frame has no vertical mode during column uplift. The sudden change in boundary condition does happen, but no column vibration is triggered. Hence, no oscillation at the period $T_{u,v}$ can be seen for the base shear with the SDOF model.

To further investigate the influence of the vertical masses, the G-CRBF model was analyzed in a modified version, referred to as G-CRBF-NM, in which m_v was set equal to 0, in order to neglect the vertical inertia forces induced by column uplift and impact. Fig. 4 details the comparison of the two studied versions of the G-CRBF model for the same ground motion presented in Fig. 3. Fig. 4b and e detail the vertical velocity of the column bases, respectively for the G-CBRF and the G-CRBF-NM models. The results were filtered with

a low-pass 10 Hz filter to ease the readability of the figures. Fig. 4 c and g detail the base shear computed from the horizontal node reaction and the brace axial loads. Figs. 4d and h plot the inertia forces generated by the horizontal mass at the roof level. In each model, these inertia forces were equal to the base shear.

In both models, peaks of positive (upwards) velocity occur when column uplift starts. Larger values of peak velocity can be observed in the frame modelled with vertical masses. For the G-CRBF model, the larger the positive velocity, the larger the peak value of the base shear demand. The amplitude of the oscillation of the force demands at period $T_{u,v}$ described in Fig. 3 is consequently related to the vertical velocity at which the column uplifted. In Fig. 4d, for both models, peaks of the base shear and the horizontal mass acceleration coincide with peaks of positive vertical velocity of the column base at the time column uplift initiates.

Altogether, the results presented in Figs. 3 and 4 show that the sudden change in boundary condition at the base of the rocking columns induce vibrations of the vertical mass carried by the columns. The vibrations are proportional to the velocity at which the columns uplift from the foundation. These vibrations induce additional force demands in the columns that are also transferred to the braces and the horizontal mass. These additional forces only occur when vertical masses are present at the column top nodes.

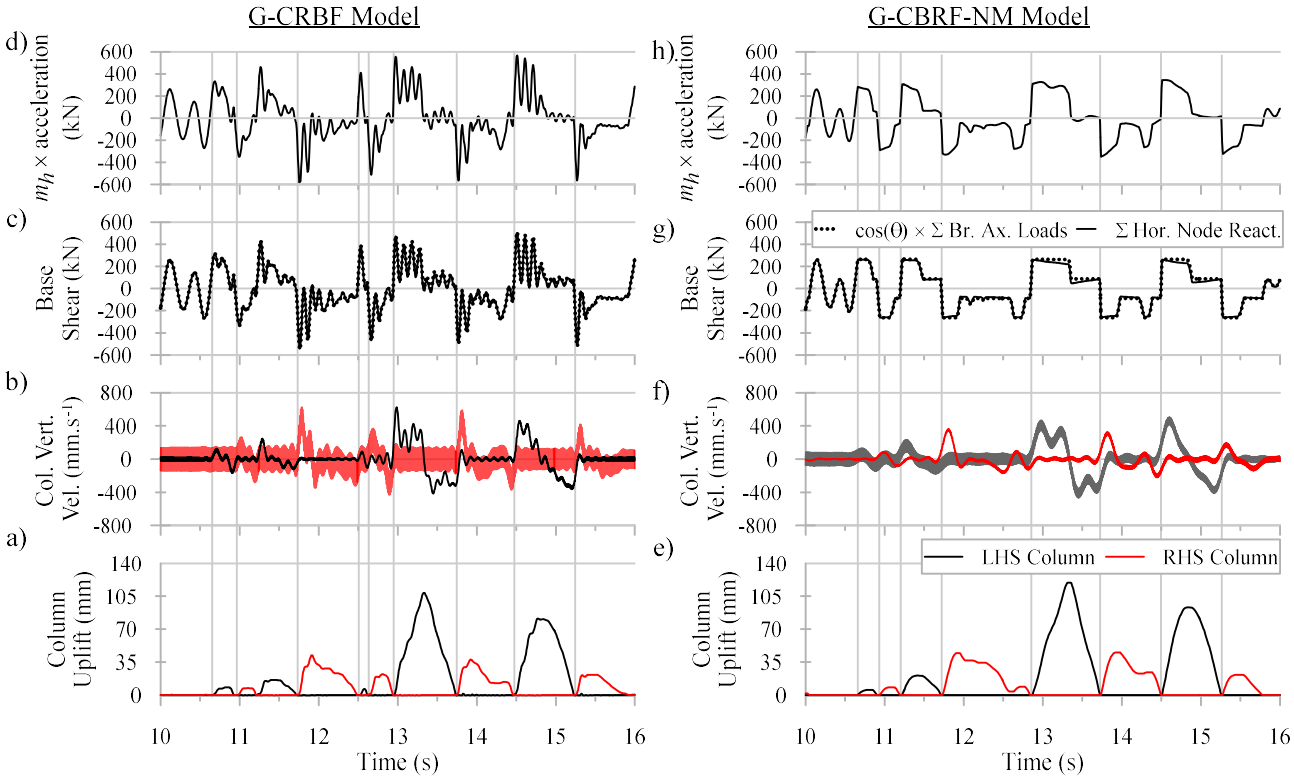

Fig. 4 Influence of the vertical masses in the two G-CRBF models: a) & e) Column uplift; b) & f) Column base vertical velocity; c) & g) Base shear; d) & h) Inertia force from the horizontal mass.

4. Response to ground motion suite

The results from the remaining 10 ground motions listed in Table 1 were examined to confirm the findings of Section 3. Fig. 5 presents the ratio of the peak responses computed with the G-CRBF model to those computed with the SDOF model for the roof displacement, base shear and vertical base reaction.

Fig. 5a shows that, on average, roof displacements from the G-CRBF model are reduced by 13% compared to those given by the SDOF model, with a standard deviation of 0.043. In Fig. 5b, it can be seen that peak base shears increase by a factor of 2.30, on average, compared to the V_R value predicted by the SDOF model, with amplification factors varying from 2.04 to 2.80. Fig. 5c shows that the average vertical base

reaction in the G-CRBF model is amplified by a factor of 2.58 relative to the SDOF value, with ratios ranging from 2.15 to 3.15. In all analyses, the maximum reaction from the SDOF model corresponds to the value obtained from static when the base shear reaches V_R. Altogether, these results from the suite of ground motions confirm the need to consider the effects of the inertia forces induced by the vertical masses to accurately predict the displacement and force demands in single-storey G-CRBFs.

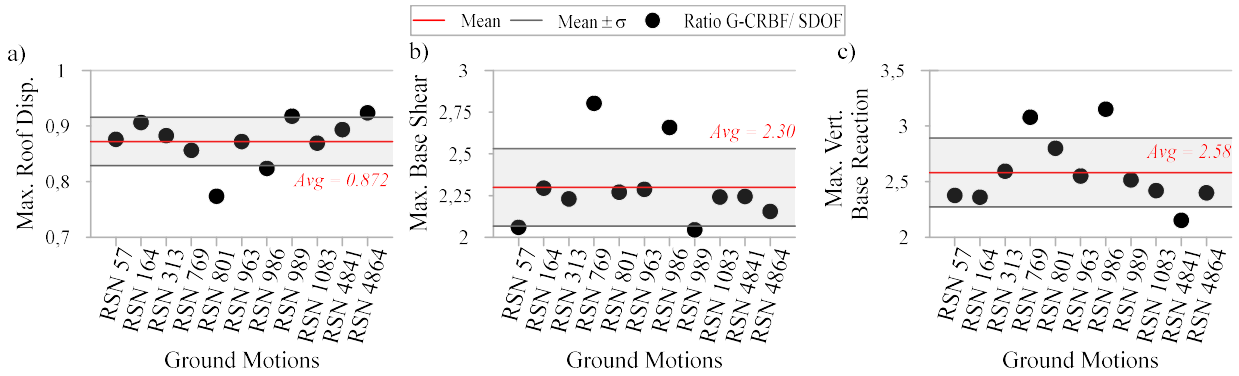

Fig. 5 Relative G-CRBF / SDOF response of the models to a suite of ground motions; a) Roof displacement; b) Horizontal base shear; c) Vertical base reaction.

5. Comparison for multi-storey buildings

The study presented in the previous sections was extended to examine vertical mass effects in 2- to 5-storey buildings. Fig. 6 presents the numerical models considered in this phase of the study.

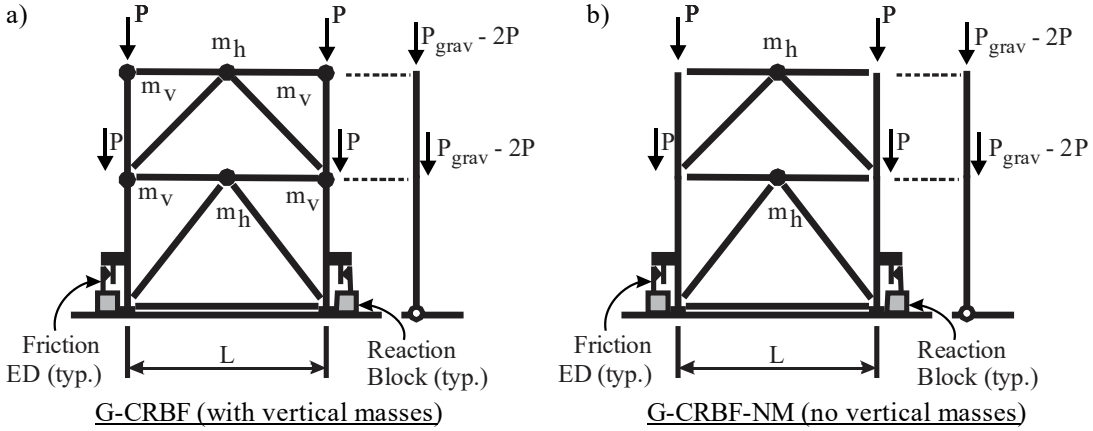

Fig. 6 Multi-storey analyses numerical models, 2-storeys configuration: a) G-CRBF model; b) G-CRBF-NM model

The G-CRBF frame, shown in Fig. 6a, is built with the same elements as described in Section 2. The second model used for comparison is the G-CRBF-NM model introduced in Section 3. Compared to the SDOF model used in Section 2, the G-CRBF-NM model was found more suitable for multi-storey structures as it can predict lateral higher mode response and vertical mass effects could then be isolated by comparing its response to that obtained with the G-CRBF model [17]. The building plan presented in Fig. 1 and the applied gravity loads were replicated at each storey level. The height of the first storey was set equal to 5.4 m, and the height of the other storeys was 4.0 m. For each frame, the cross-section areas of the frame members were modified to match the fundamental period value prescribed in NBC 2015 as a function of the building height. To simplify the study, the numerical model built for the single-storey analysis was used. $F_s = 0.5\,P$ was kept, as well as the same base overturning moment capacity, for all buildings studied. Therefore, the scaling of the ground motions was modified so that the seismic demand would be consistent with the NBC spectrum assuming the same R

value for all buildings. Mass-proportional damping was applied to the two models assuming a damping ratio of 3% in the first two horizontal modes of the fixed-base frame. As in the previous section, no stiffness-related damping was assigned to model.

Table 2 presents the fundamental periods of vibration of the two studied models for the fixed-base condition. As can be seen, the fundamental periods of the G-CRBF model are slightly longer than those of the G-CRBF-NM model, with a maximum increase of 6 %. This difference is due to the vertical masses present in the first model. For the G-CRBF model, the period of the vertical modes in the fixed base condition (T_c) and uplift conditions ($T_{u,v}$) are also given in the table.

Table 2 Periods of vibration (s) of the two studied numerical models

Number of Storeys	G-CRBF Model - Fixed Base					G-CRBF Rocking		G-CRBF-NM Model - Fixed Base				
	Mode 1	Mode 2	Mode 3	Mode 4	Mode 5	$T_{u,v}$	T_c	Mode 1	Mode 2	Mode 3	Mode 4	Mode 5
1	0.343	-	-	-	-	0.0975	0.050	0.343	-	-	-	-
2	0.467	0.179	-	-	-	0.091	0.056	0.466	0.176	-	-	-
3	0.668	0.250	0.130	-	-	0.106	0.058	0.666	0.246	0.130	-	-
4	0.866	0.293	0.146	0.109	-	0.114	0.053	0.864	0.289	0.145	0.108	-
5	1.081	0.325	0.161	0.113	0.100	0.119	0.049	1.078	0.322	0.160	0.112	0.094

Fig. 7 presents the results for the two-storey building under ground motion #6 for the two models studied. As shown in Fig. 7b, the G-CRBF-NM exhibits higher peak column uplifts than the G-CRBF model, but the differences significantly reduced compared to the single-storey building case. At t = 13.34 s, the maximum uplift in the G-CRBF-NM is 73 mm compared to 70 mm for the G-CRBF model, which represents 3 % increase. The same observation can be drawn for the roof drifts, as shown in Fig. 7c. The base shear demands are presented in Fig. 7d. Assuming a first mode response of the structure, the static value of the rocking base shear is equal to V_R=359 kN, assuming NBC vertical distribution of lateral seismic loads [15]. The results show a similar behaviour between the two studied models, but the peak values of the base shear observed with the G-CRBF model are higher than the ones obtained with the G-CRBF-NM model. As is detailed in Fig. 7g, for the time frame presented, the peak base shear is reached at t = 13.2 s for both models, with values equal to 571 and 617 kN for G-CRBF-NM and G-CRBF models, respectively. This represents an 8% increase due to the vertical masses, and 71% increase compared to the static value V_R. Fig. 7g also shows that the base shear history from the G-CRBF model displays two different periods of oscillation which correspond to $T_{u,h,2}$ and $T_{u,v}$, alternatively. $T_{u,h,2}$ refers to the second horizontal mode of the frame during uplift. Figs. 7e and f show the history of the axial force in the LHS column first storey for both models. As shown, the two columns exhibit an overall similar behaviour during rocking, though higher forces can be observed for the G-CRBF model. Otherwise, significant increase in compression loads can be noted at time of impacts due to the vertical masses. At t = 13.82 s, the impact of the LHS column triggers a maximum compression load of 667 kN, which is 2.66 times the static value of 2 P. As noted, the forces in the columns of the G-CRBF-NM model are governed by higher modes with period $T_{u,v}$ during the rocking cycles. When the column is in contact with the foundation, the vertical masses oscillate at the period T_c. As shown in Fig. 7h, which displays the hysteretic base shear vs. roof drift curve, higher modes significantly contribute to the overall behaviour of the frame and induce higher than V_R peak base shears. Figs. 8a and b present a summary of the results of the multi-storey analyses performed for the whole suite of ground motions listed in Table 1. Fig. 8a displays mean ratios of the maximum values obtained in the G-CRBF and G-CRBF-NM models for the roof drift, horizontal base shear and vertical base reaction. Standard deviation values are plotted as error bars at the top of each bar. In all cases, the G-CRBF model with vertical masses experienced smaller roof drifts compared to the G-CRBF-NM model, the reduction being more significant for the single-storey building (13 %) than for the multi-storey

buildings (3% on average). No significant differences in drift reduction can be observed between the multi-storey buildings studied.

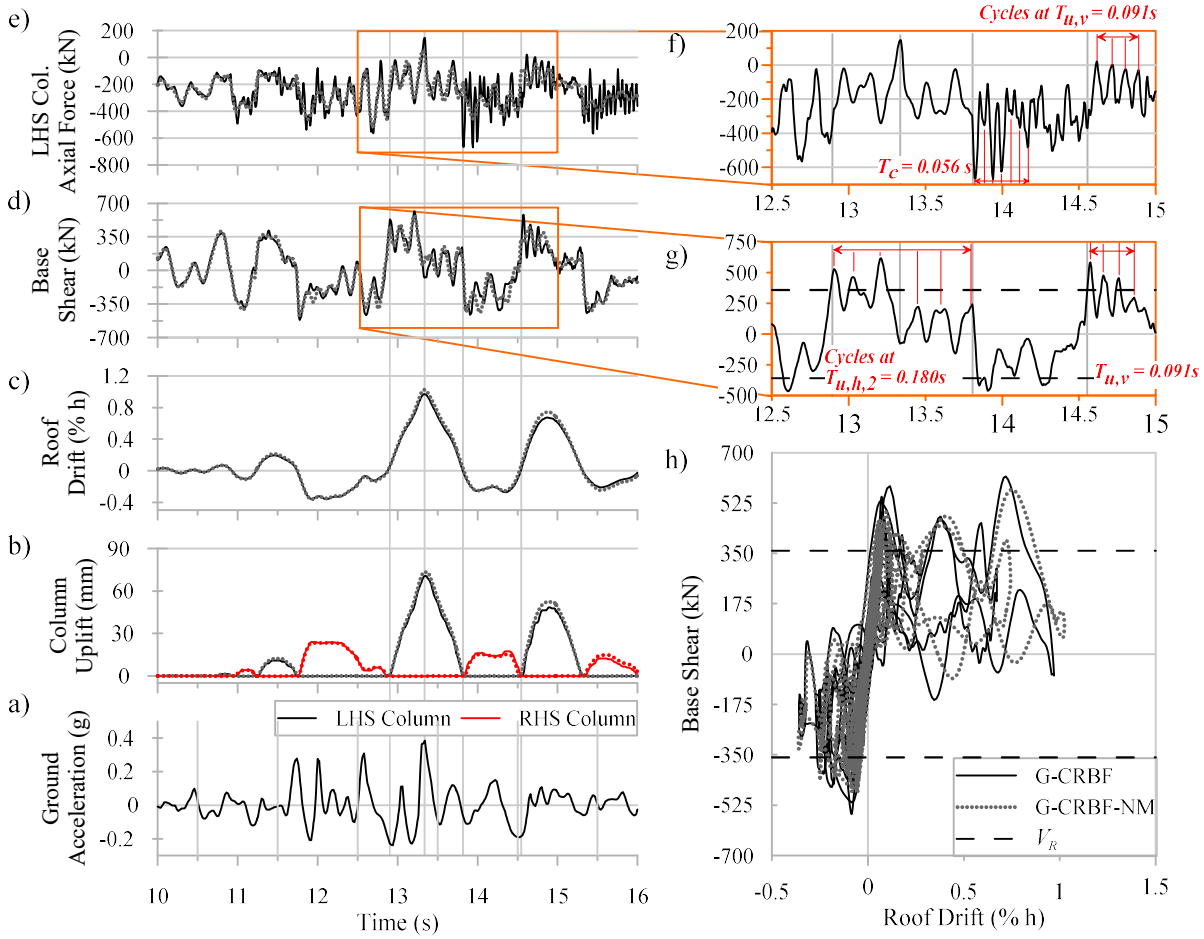

Fig. 7 Response history analysis results in the multi-storey configuration: comparison between the response of the G-CRBF and G-CRBF-NM models: a) Ground motion; b) Column uplift; c) Roof drift; d) & g) Base shear; e) & f) Column axial load; h) Base shear *vs.* roof drift hysteresis.

In terms of base shear and vertical base reaction, the results show that the demand amplification in the G-CRBF model with vertical masses is maximum for the single-storey building and becomes less significant as the number of storeys increases. The base shear ratios significantly decrease for the 2-storey buildings (1.09 in lieu of 2.30 for the single-storey building) and then tends towards 1.0 for the 3- to 5-storey buildings, with a coefficient of variation less than 11%. The vertical base reaction ratio also drops from 2.58 to 1.64 between the single- and 2-storey buildings and tends towards 1.30 for 3-storey and taller buildings. Overall, these results show that the influence of the vertical masses tends to decrease as the number of storeys of the buildings studied increase. Fig. 8b displays the ratios between the means of the maximum base shear and vertical reaction values from the two models and the static values. For the base shear, the value from G-CRBF-NM model shows steadily increasing demand compared to the static value due to higher lateral mode effects. The ratios from the G-CRBF model are higher for the single-storey structure but then become similar to the G-CRBF-NM model, indicating that the influence of vertical masses on base shear, which is significant for single-storey buildings, becomes less important for taller frames, due to the growing influence of lateral higher modes. Hence the influence of the vertical mode relatively reduces as the number of stories increases. In Fig. 8b, it can also be seen that peak vertical base reactions in the G-CRBF-NM model are essentially equal to the static value. Higher values are observed with the G-CRBF model, especially for the single- and 2-storey frames. This confirms that vertical masses must be considered when modelling G-CRBFs for low-rise buildings.

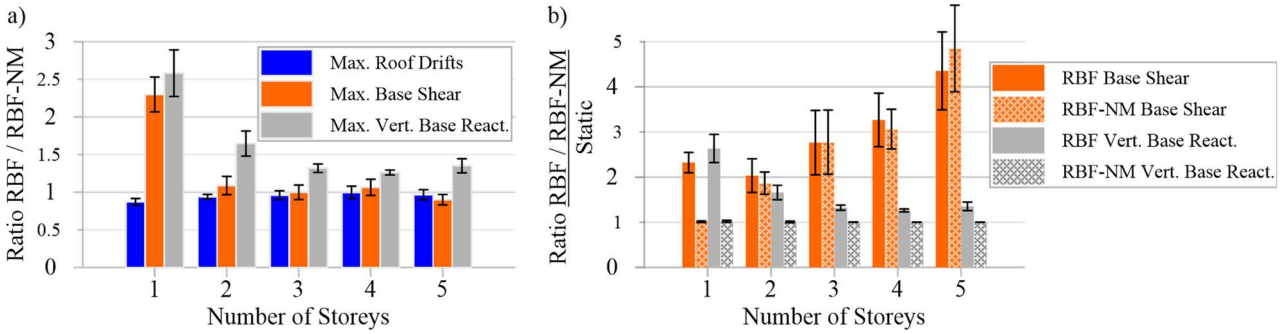

Fig. 8 Results of the multi-storey analyses performed on G-CRBF and G-CRBF-NM models for the 11 selected ground motions: a) Ratio between G-CRBF and G-CRBF-NM results; b) Ratio to static results

6. Conclusion

A numerical study was performed to assess the influence of the vertical masses on the seismic behaviour of gravity-controlled rocking braced frames, with focus to the inertia forces induced by the uplift of the braced frames and by the impacts between the columns and their foundation upon rocking. First, a single-storey G-CRBF building was studied using two different models: 1) 2D-frame model in which vertical masses corresponding to the gravity loads carried by the columns were assigned to the column top nodes, and 2) SDOF model without vertical masses. Nonlinear response history analyses were performed in Opensees for representative ground motions. The results showed that the drifts experienced by the G-CRBF modelled with vertical masses were, on average, equal to 0.83 times the values obtained with the SDOF model., suggesting that SDOF model predictions would overestimate the drift demands for single-storey G-CRBFs.. The results however showed that base shears and brace axial loads were increased when including vertical masses in the model, as a result of vertical mode response triggered upon column uplift. Column axial loads and vertical base reactions were also increased with vertical masses, due to column impact combined with vertical dynamic responses in the uplifted and fixed base conditions. Neglecting vertical masses in G-CRBF analysis would therefore underestimate force demands in the braced frame members.

When expanded to multi-storey buildings, vertical mass effects were assessed by comparing the response obtained from two identical 2D frame models except that only one model included vertical masses at beam-to-column nodes. For the selected ground motions and buildings studied, the results showed that drift reduction due to the presence of the vertical masses becomes less significant as the number of storeys increases. Amplification of the base shears and vertical base reactions observed for single storey G-CRBF was less pronounced for the taller structures. For 3-storey and taller buildings, peak base shears from both numerical models were found to be equivalent. For these buildings, vertical base reactions were however amplified by a factor of 1.30, on average, when assigning vertical masses to the frame model. From these results, it can be concluded that vertical masses have limited effects on the drifts, base shears and member force demands for G-CRBFs used in mid-rise buildings having 3 or more storeys. The influence of the vertical mode relatively reduces as the number of stories increases, due to the growing influence of lateral higher modes. Vertical masses should however be considered in the seismic analysis of lower G-CRBFs to properly assess displacement and force demands in G-CRBFs used in lower buildings.

Additional research is needed on more G-CRBF buildings to expand the conclusions drawn from this study. The vertical component of the ground motions should be included in future studies. The numerical models should include the floor structures supported by the rocking columns so that this additional flexibility be considered in the response and dynamic effects on beams and beam connections can be assessed. The numerical model should also consider the possible restraining effects of composite floor and roof slabs on the rocking response.

7. Acknowledgements

Funding for this research was provided by the Fonds de Recherche du Québec - Nature et technologies (FRQNT) of the Government of Quebec, Canada, and the Centre d'études interuniversitaire des structures sous charges extrêmes (CEISCE).

8. References

[1] Priestley M. JN, Evison RJ, Carr AJ (1978): Seismic response of structures free to rock on their foundations. *Bulletin of the New Zealand National Society for Earthquake Engineering*, **11** (3), 141-150.

[2] Midorikawa M, Azuhata T, Ishihara T, Wada A (2006): Shaking table tests on seismic response of steel braced frames with column uplift. *Earthquake Engineering and Structural Dynamics*, **35** (14), 1767-1785.

[3] Ma X, Deierlein G, Eatherton M, Krawinkler H, Hajjar J, Takeuchi T, Kasai K, Midorikawa M, Hikino T (2010): Large-scale shaking table test of steel braced frame with controlled rocking and energy dissipating fuses. *9th US and 10th Canadian Conference on Earthquake Engineering*, Toronto, ON, Canada, Paper No 1330.

[4] Wiebe L, Christopoulos C, Tremblay R, Leclerc M (2013): Mechanisms to limit higher mode effects in a controlled rocking steel frame. 1: Concept, modelling, and low-amplitude shake table testing. *Earthquake Engineering and Structural Dynamics*, **42** (7), 1053-1068.

[5] SCNZ (2015): *SCNZ-110:2015, Design guide for controlled rocking steel braced frames,* Steel Construction New Zealand Incorporated, Manukau City, New Zealand.

[6] Roke, D, Sause, R, Ricles, JM, Gonner, N (2009): Design concepts for damage-free seismic-resistant self-centering steel concentrically braced frames. *Structures Congress 2009: Don't Mess with Structural Engineers: Expanding Our Role* (pp. 1-10).

[7] Eatherton MR., Ma X, Krawinkler H, Mar D, Billington S, Hajjar JF, Deierlein GG (2014): Design concepts for controlled rocking of self-centring steel-braced frames. *Journal of Structural Engineering*, **140** (11), 04014082.

[8] Wiebe L, Christopoulos C (2014): Performance-based seismic design of controlled rocking steel braced frames. I: Methodological framework and design of base rocking joint. *Journal of Structural Engineering*, **141** (9), 04014226.

[9] Zhang C, Steele TC, Wiebe LD, (2018): Design-level estimation of seismic displacements for self-centring SDOF systems on stiff soil. *Engineering Structures*, **177**, 431-443.

[10] Mottier P, Tremblay R, Rogers C (2018): Seismic retrofit of low-rise steel buildings in Canada using rocking steel braced frames. *Earthquake Engineering & Structural Dynamics*, **47** (2), 333-355.

[11] Mottier P, Tremblay R, Rogers CA (2018): Shake Table Test of a Half-Scale 2-Storey Steel Building Seismically Retrofitted Using Rocking Braced Frame System. *Proc. STESSA 2018 – 9th International Conference on the Behaviour of Steel Structures in Seismic Areas*, Christchurch, New Zealand.

[12] Tran BT, Kasai K, Sato T, Oohara K, Shao L (2004): JSSI manual for building passive control technology part-7 stepping column system. *Proc. 13th World Conference on Earthquake Engineering*, Vancouver, BC, Canada, Paper no. 5059**.**

[13] OpenSees (2015): Open system for earthquake engineering simulation v2.4.5 [computer software]. http://opensees.berkeley.edu/

[14] Tremblay R, Atkinson GM, Bouaanani N, Daneshvar P, Léger P, Koboevic S (2015): Selection and scaling of ground motion time histories for seismic analysis using NBCC 2015. *11th Canadian Conference on Earthquake Engineering*, Victoria, BC, Canada.

[15] NRCC (2015): *National Building Code of Canada 2015*, 14th ed. National Research Council of Canada, Ottawa, Ontario.

[16] Yim C S, Chopra,A K (1983). Effects of transient foundation uplift on earthquake response of structures, Report No. UCB/EERC 83-09. *Earthquake Engineering Research Center, University of California, Berkeley*

[17] Wiebe L, Christopoulos C (2009) Mitigation of higher mode effects in base-rocking systems by using multiple rocking sections. *Journal of Earthquake Engineering*, **13** (S1), 83-108.

